Supporting Information

Synthesis of single crystalline two-dimensional transition-metal phosphides via salt-templated method

Tianqi Li,[a] *Hongrun Jin,*[a] *Zhun Liang,*[b] *Liang Huang,*[a] *Yucheng Lu,*[a] *Huimin Yu,*[a] *Zhimi Hu,*[a] *Jiabin Wu,*[a] *Bao Yu Xia,*[c] *Guang Feng,*[b] *Jun Zhou*[a]*

[a]Wuhan National Laboratory for Optoelectronics and School of Optical and Electronic Information, Huazhong University of Science and Technology, Wuhan 430074, China

[b]State Key Laboratory of Coal Combustion, School of Energy and Power Engineering, Huazhong University of Science and Technology, Wuhan 430074, Hubei, P. R. China.

[c] Key laboratory of Material Chemistry for Energy Conversion and Storage (Ministry of Education), Hubei Key Laboratory of Material Chemistry and Service Failure, School of Chemistry and Chemical Engineering, Huazhong University of Science and Technology, Wuhan 430074, Hubei, P. R. China.

* Correspondence author: jun.zhou@mail.hust.edu.cn

1. Experiment Details

Synthesis of 2D Co_2P. Firstly, $Co(NO_3)_2 \cdot 6H_2O$ (0.002 mol) was dissolved into ethanol (40 ml). The above precursor solutions were added to 500 g of KCl powder followed by drying at 60 ℃ with stirring. Secondly, $(NH_4)_2HPO_4$ (0.39 g) was dispersed in mixed solvent of deionized water (10 ml) and ethanol (10 ml) with some salt powders added to forbid dissolution of salt templates. The Co@KCl powders were covered with $(NH_4)_2HPO_4$ solution in the same way. The resulting mixture was transferred into alumina crucible which was placed at the center of tube furnace. Under the protection of Ar/H_2 atmosphere, the temperature was increased to 700 ℃ with the rate of 1 ℃ per minute and kept for 3 hours. After being cooled, the annealed product was repeatedly washed with deionized water to remove the salt templates. In order to prevent oxidation of the products in the washing process, N_2 was bubbled into deionized water constantly to exclude oxygen. The 2D Co_2P nanosheets were obtained by vacuum filtration. The resulting products were transferred into vacuum drying oven to dry overnight at 50 ℃ for further characterization.

Synthesis of 2D MoP_2. 2D MoP_2 was synthesized through an identical procedure but $(NH_4)_6Mo_7O_{24} \cdot 4H_2O$ and NaCl were used as metal precursor and salt templates, respectively. Meanwhile, citric acid (0.004 mol) was dissolved into ethanol (50 ml) and the as-obtained solution was added to salt powders. The resulting mixture was preannealed at 500 ℃ in air before further annealed at 700 ℃ in the Ar/H_2 atmosphere.

Synthesis of 2D $Ni_{12}P_5$. The procedure was identical with the synthesis of 2D Co_2P, but $Ni(NO_3)_2 \cdot 6H_2O$ was used as metal precursor.

Synthesis of 2D WP_2. The procedure was identical with the synthesis of 2D MoP_2, but $(NH_4)_6H_2W_{12}O_4 \cdot nH_2O$ was used as metal precursor.

Synthesis of Co_2P nanoparticles. The Co_2P NPs are synthesized by the same method of 2D Co_2P without salt templates. In detail, we mixed $Co(NO_3)_2 \cdot 6H_2O$ solution and $(NH_4)_2HPO_4$ solution in the Co/P atom ratio of 2:1. After vacuum filtration, the precursors are annealed at 700 ℃ for 3 hours under the protection of Ar/H_2 atmosphere. The resulting products were transferred into vacuum drying oven

to dry overnight at 50 ℃ for further characterization.

Electrochemical measurements. Electrochemical measurements were evaluated by CHI 660E electrochemical workstation. The counter and reference electrodes selected were graphite rod and saturated calomel electrode (SCE), respectively. A glassy carbon electrode (GCE, 5 mm in diameter) covered by catalyst materials was used as the working electrode. The electrolyte was 0.5 M H_2SO_4 solutions. Typically, 5 mg 2D TMPs were suspended in mixed solvent of deionized water (200 μl) and isopropyl alcohol (800 μl), then 20 μl Nafion solution (5.0 wt.%. Nafion in isopropyl alcohol) was added to the as-obtained solution to form a homogeneous ink assisted by sonication. 10 μl of the ink was loaded onto GCE by a micropipette and dried in ambient temperature. Before measurements, the samples were repeatedly swept from 0.05 to 0.35 V (vs. RHE) in the electrolyte until a steady voltammogram curve was obtained. The LSV curves were scanned from 0 to -0.7 V (vs. RHE) at a scan rate of 5 mV s^{-1}. Electrochemical Impedance Spectroscopy (EIS) was measured at -30 mV (vs. RHE) with the AC voltage amplitude of 5 mV and the frequency range of 0.1-106 Hz.

Characterization. The morphology, microstructure and valence state of the samples were characterized by field-emission scanning electron microscope (FEI Nova 450 Nano), high-resolution transmission electron microscopy (FEI Titan G2 60-300), Atomic force microscope (Shimadzu), X-ray photoelectron spectrum (ESCALab250). The powder X-ray diffraction (X'Pert Pro, PANanalytical) measurements were taken at 40 kV accelerating voltage and a 40 mA current with Cu Kα radiation. For the AFM measurements, the samples were dropped on SiO_2/Si and dried at room temperature.

2. Supplementary Notes

Supplementary Note 1: Growth mechanism of MoP_2

According to the growth mechanism, the lattice mismatch between (010) plane of MoP_2 (c-axis is 0.4984 nm) and (001) plane of NaCl (a-axis is 0.5620 nm) is 12% (Fig. 3d), which is against to the surface growth. However, the orthorhombic structure

of MoP_2 and large b axis take conducive to formation of 2D MoP_2 morphology, because thin layered morphology (Figure S3) usually has larger b axis than the bulk. Owing to atomic thin film of MoP_2 and the large lattice mismatch between MoP_2 and NaCl, there will be some lattice distortion in MoP_2 leading to no (020)/(040)/(060)/(080) peak exist in the mixture of MoP_2@NaCl XRD pattern even at slow scan (Figure S4). After removing the NaCl template, the MoP_2 exposes out (010) crystal plane caused by the nanosheets stack together.

Supplementary Note 2: Active sites calculation

The active sites calculation of Pt/C is based on CO stripping experiment.[1,2] The oxidation peak at 0.78 V can be attributed to the CO stripping peak. The number of active sites in Pt/C was further calculated to 0.4 mmol/g.

In order to calculate the active sites of 2D Co_2P, we design a catalyst poisoning method. Firstly, we added KSCN to poison Pt/C catalyst. According to polarization curves, the onset potential of Pt/C shifted to -30 mV. Moreover, the under potential deposition of hydrogen on Pt is not clear. While it is difficult to assign the observed peaks to a given redox couple, the total number of active sites could be calculated from reported method. The total charge with removing electrochemical double layer capacitance has been integrated from CV curves. The number of active sites in Pt/C was calculated to 0.428 mmol/g which is close to the CO stripping method.

The active sites calculation of 2D Co_2P is based on integral of CV curves.[3] The onset potential of 2D Co_2P for HER shifted to -80 mV. Similarly, the number of active sites could be calculated from integral of CV curves, which is 0.308 mmol/g for 2D Co_2P. The number of active sites of Co_2P nanoparticle is 0.165 mmol/g.

Supplementary Note 3: The calculation of TOF

The calculation of TOF is based on the following equation:

$$TOF=I/(2Fn)$$

where I is the current (A) during linear sweep measurement, F is the Faraday constant (C/mol), n is the number of active sites (mol). The factor 1/2 is based on the consideration that two electrons are required to form one hydrogen molecule.

3. Supplementary Figures:

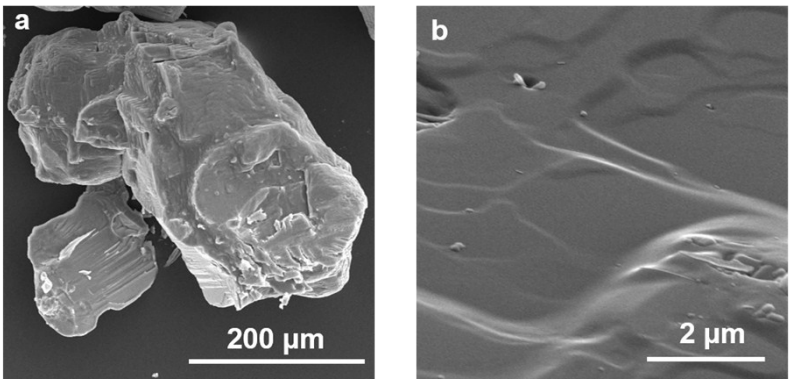

Figure S1. (a) and (b) The SEM images of KCl coating with 2D Co_2P.

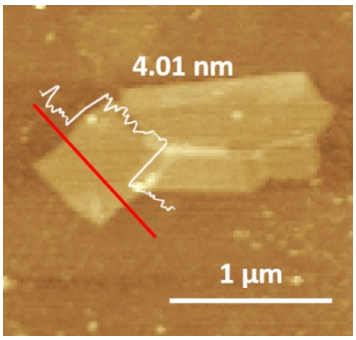

Figure S2. The AFM image of 2D Co_2P. The thickness of 2D Co_2P is 4 nm.

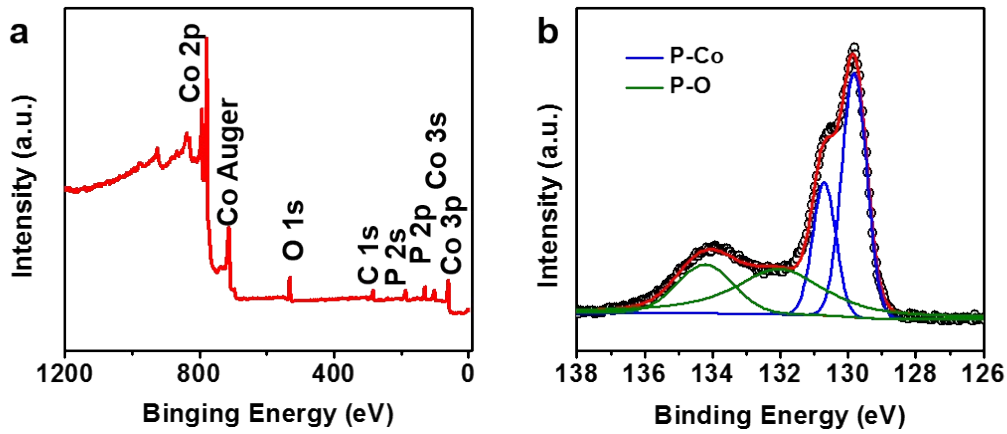

Figure S3. XPS spectra of Co_2P. Survey spectra (a) and P 2p (b). The peaks of P 2p are divided into four peaks, corresponding to P-Co 2p3/2 (129.8 eV), P-Co 2p1/2 (130.7 eV), P-O 2p1/2 (132.0 eV) and P-O 2p3/2 (134.2 eV).

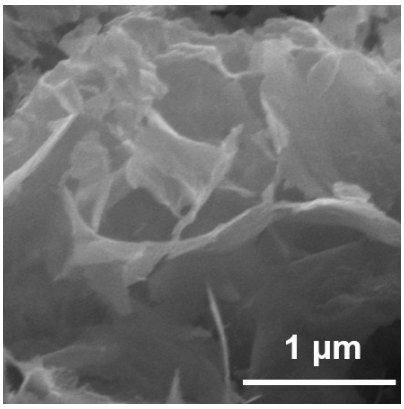

Figure S4. SEM image of 2D MoP_2.

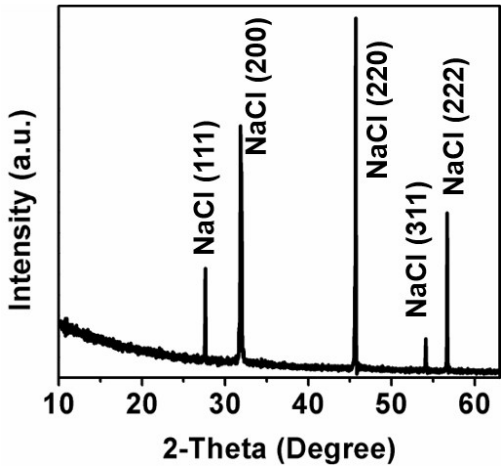

Figure S5. XRD pattern of 2D MoP_2 on NaCl. All of the diffraction peaks belong to NaCl.

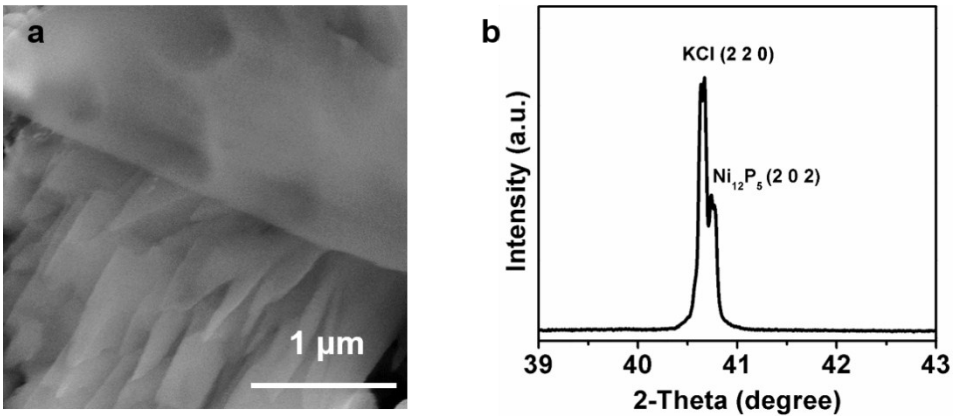

Figure S6. (a) The SEM images of 2D $Ni_{12}P_5$. (b) The XRD pattern of 2D $N_{12}P_5$ on KCl.

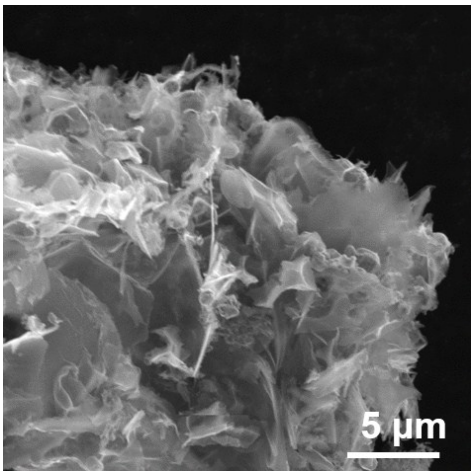

Figure S7. SEM image of 2D WP_2.

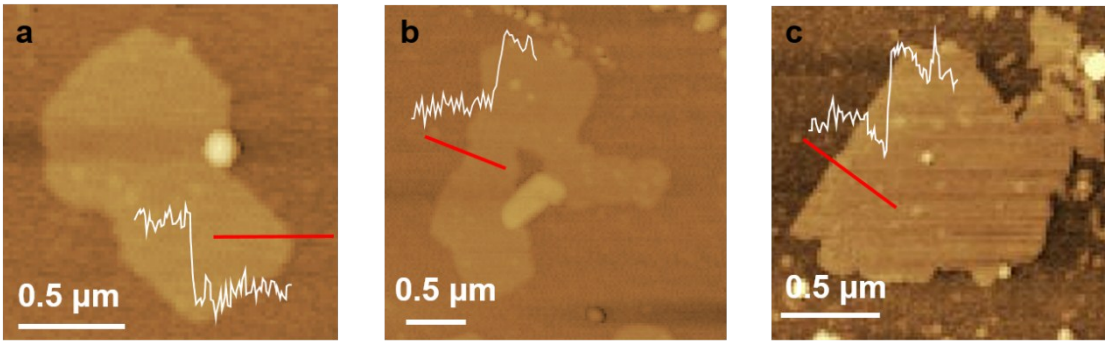

Figure S8. AFM images of 2D TMPs. According to the AMF images, the thickness of 2D MoP_2 (a), $Ni_{12}P_5$ (b) and WP_2 (**c**) is ~2.5 nm, ~ 1.8 nm and ~ 2.3 nm, respectively. Scale bar, 0.5 μm.

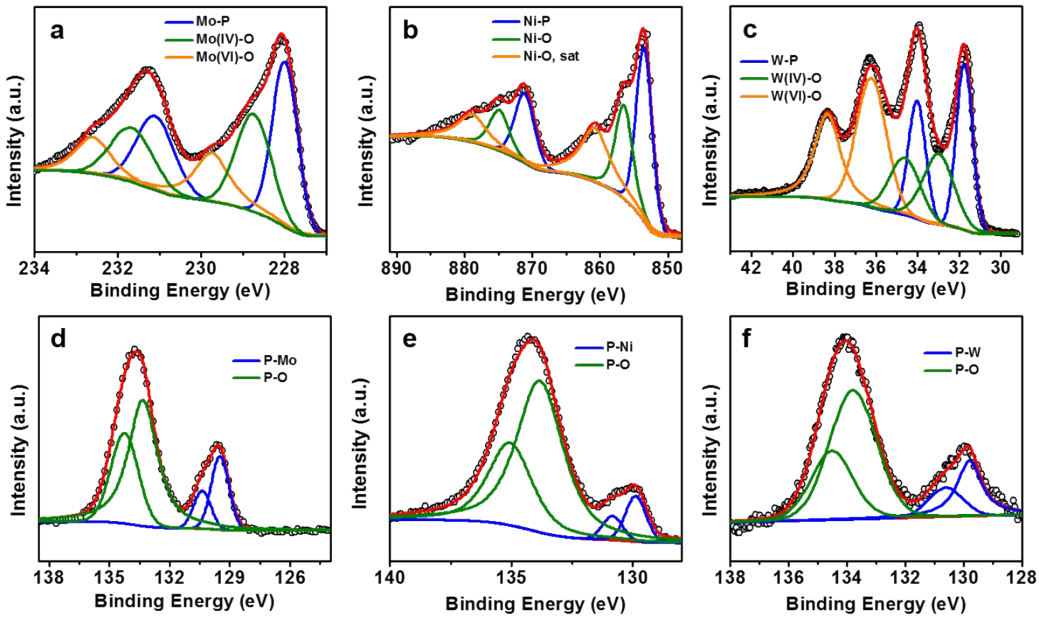

Figure S9. XPS of 2D TMPs (MoP_2, $Ni_{12}P_5$ and WP_2). For these 2D TMPs, all their surface had metal-oxygen and metal-phosphorus bonds. In detail, the peaks of Mo-P bond (a), Ni-P bond (b) and W-P bond (c) could be analyzed by Mo 3d (228.0 eV for Mo $3d_{5/2}$, 231.2 eV for Mo $3d_{3/2}$), Ni 2p (853.6 eV Ni $2p_{3/2}$, 871.2 eV for Ni $2p_{1/2}$) and W 4f (31.78 eV for W $4f_{7/2}$, 34.08 eV for W $4f_{5/2}$), respectively. Analogous to Co_2P, MoP_2, $Ni_{12}P_5$ and WP_2 also have partial oxidization on the surface. We believe the oxidation layers of these 2D TMPs may help them stably disperse in water. The XPS spectra of P 2p. (d) The peaks of 2D MoP_2 are divided into four peaks, corresponding to P-Mo $2p_{3/2}$ (~129.5 eV), P-Mo $2p_{1/2}$ (~130.3 eV), P-O $2p_{1/2}$ (~133.3 eV) and P-O $2p_{3/2}$ (~134.2 eV). (e) The peaks of 2D $N_{12}P_5$ are divided into four peaks, corresponding to P-Mo $2p_{3/2}$ (~129.5 eV), P-Mo $2p_{1/2}$ (~129.8 eV), P-O $2p_{1/2}$ (~133.8 eV) and P-O $2p_{3/2}$ (~135.0 eV). (f) The peaks of 2D WP_2 are divided into four peaks, corresponding to P-Mo $2p_{3/2}$ (~129.8 eV), P-Mo $2p_{1/2}$ (~130.6 eV), P-O $2p_{1/2}$ (~133.8 eV) and P-O $2p_{3/2}$ (~134.6 eV).

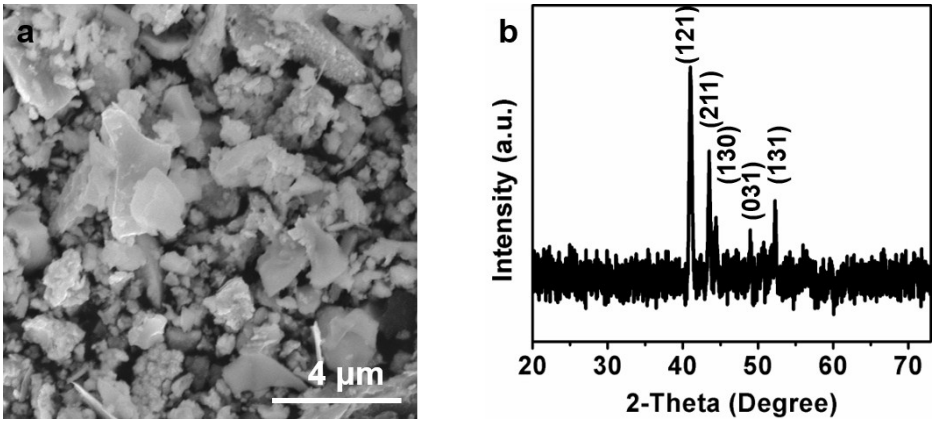

Figure S10. Co_2P synthesized on NaCl. According to SEM image (a) the morphology is particle instead of 2D nanosheet. (b) The XRD pattern of Co_2P synthesized on NaCl.

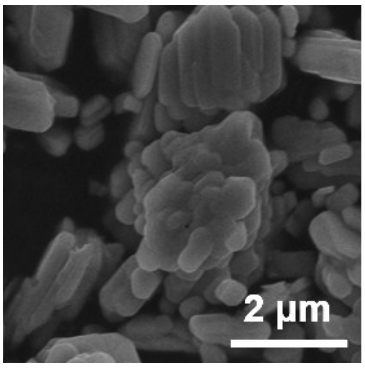

Figure S11. The SEM images of Co_2P nanoparticles.

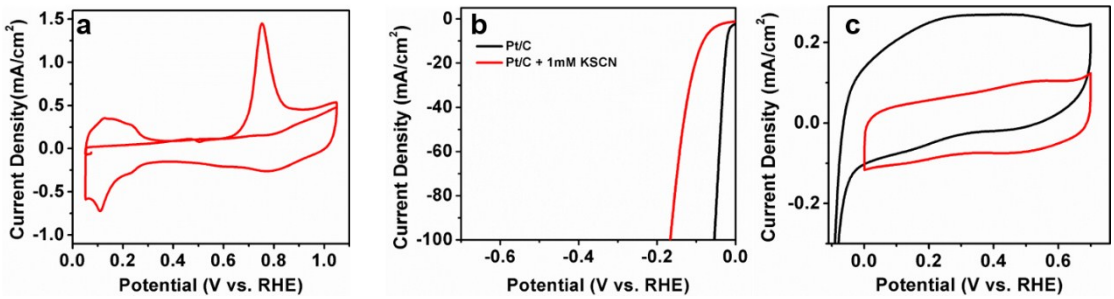

Figure S12. TOF calculation of Pt/C. (a) The CO stripping voltammetry of Pt/C in 0.5 M aq. H_2SO_4. Stripping of a monolayer of CO in the first cycle. Following cycle after the stripping of CO. (b) The linear sweep voltammetry (LSV) curves of Pt/C before and after KSCN poisoning. (c) The cyclic voltammetry (CV) curves of poisoned Pt/C with hydrogen atom absorbed.

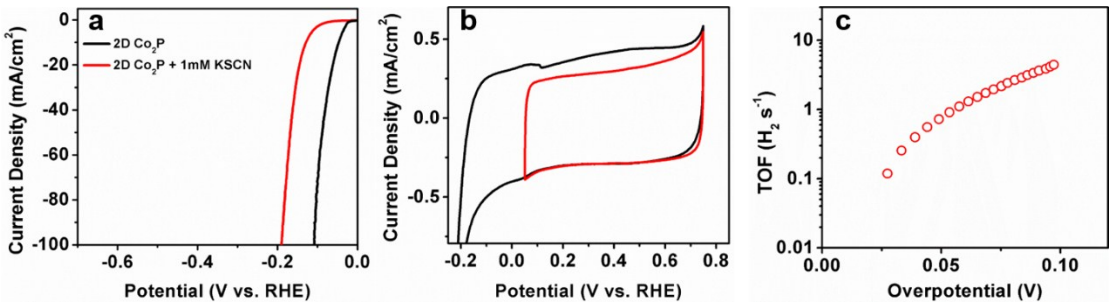

Figure S13. TOF calculation of 2D Co_2P. (a) The LSV curves of 2D Co_2P before and after KSCN poisoning. (b) The CV curves of poisoned 2D Co_2P with hydrogen atom absorbed. (c) The turnover frequency values of 2D Co_2P. The TOF of Co_2P is 0.77 s^{-1} at -50 mV (vs. RHE).

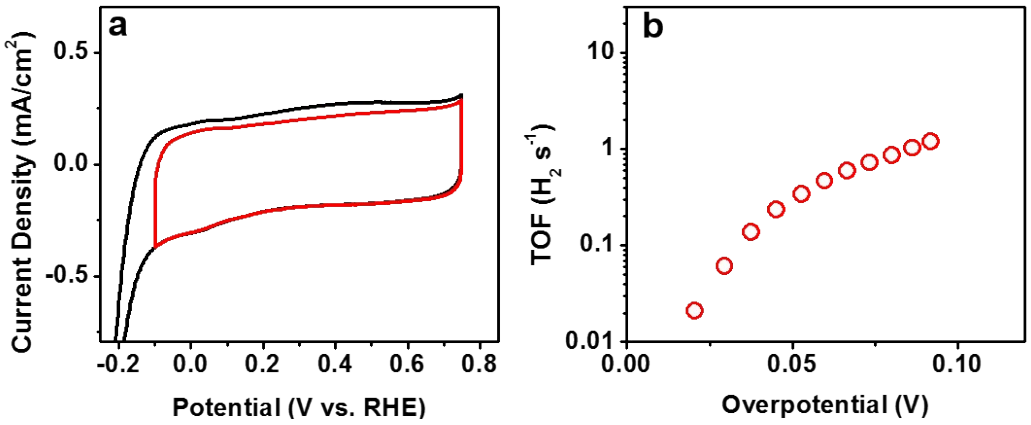

Figure S14. TOF calculation of Co_2P particles. (a) The active sites calculation of Co_2P particles is similar to that of 2D Co_2P. (b) The TOF of Co_2P Particles is 0.31 s^{-1} at - 50 mV (vs. RHE).

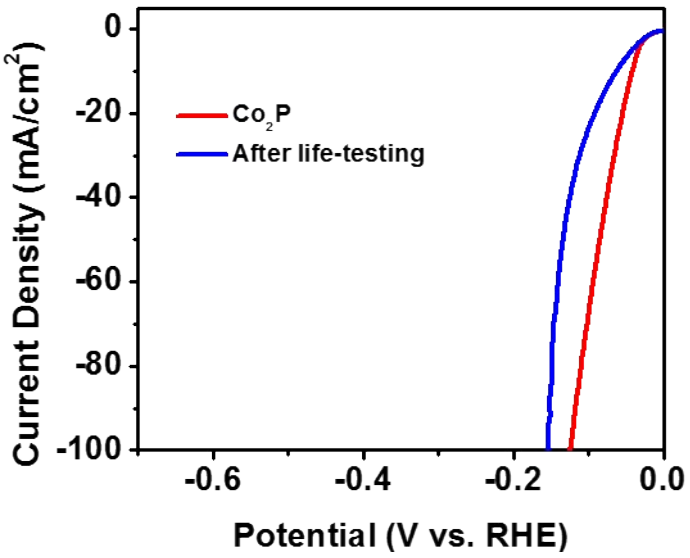

Figure S15. Durability test of 2D Co_2P. Durability test of 2D Co_2P is based on the polarization curves before and after 5000 potential cycles (50 mV/s) in 0.5 M H_2SO_4 solution from 0 V to 0.6 V (vs. RHE).

4. Supplementary Table:

Table S1. Summary of some recently reported transitional metal phosphides for HER electrocatalysts in 0.5 M H_2SO_4.

	Overpotential (mV) at 10 mA cm^{-2}	Tafel slope (mV dec^{-1})
This work	41	35
CoP [4]	85	50
CoP [5]	~120	46
Co_2P [6]	~100	50
Co_2P [7]	103	58
CoP/RGO [8]	105	50
CoP [9]	95	50
CoP [10]	67	51
CoP [11]	56	44
CoP [12]	253	73
Cu_3P [13]	143	67
FeP [14]	155	38
FeP [15]	52	49
FeP [16]	58	45
MoP|S [17]	64	50
MoP [15]	51	45
$Ni_{12}P_5$ [18]	208	75
$Ni_{12}P_5$ [19]	107	63
Ni_2P [20]	172	62
Ni_2P [18]	137	49
Ni_5P_4 [18]	118	42
WP [21]	130	69

REFERENCES

1. H. A. Gasteiger, N. Markovic, P. N. Ross and E. J. Cairns, *J. Phys. Chem.,* 1994, **98**, 617-625.
2. J. Mahmood, F. Li, S. M. Jung, M. S. Okyay, I. Ahmad, S. J. Kim, N. Park, H. Y. Jeong and J. B. Baek, *Nat. Nanotechnol.*, 2017, **12**, 441-446.
3. D. Merki, S. Fierro, H. Vrubel and X. Hu, *Chem. Sci.*, 2011, **2**, 1262-1267.
4. F. H. Saadi, A. I. Carim, E. Verlage, J. C. Hemminger, N. S. Lewis and M. P. Soriaga, *J. Phys. Chem. C*, 2014, **118**, 29294-29300.
5. H. Yang, Y. Zhang, F. Hu and Q. Wang, *Nano Lett.*, 2015, **15**, 7616-7620.
6. J. F. Callejas, C. G. Read, E. J. Popczun, J. M. McEnaney and R. E. Schaak, *Chem. Mater.*, 2015, **27**, 3769-3774.
7. M. Zhuang, X. Ou, Y. Dou, L. Zhang, Q. Zhang, R. Wu, Y. Ding, M. Shao and Z. Luo, *Nano Lett.*, 2016, **16**, 4691-4698.
8. L. Jiao, Y.-X. Zhou and H.-L. Jiang, *Chem. Sci.*, 2016, **7**, 1690-1695.
9. E. J. Popczun, C. G. Read, C. W. Roske, N. S. Lewis and R. E. Schaak, *Angew. Chem. Int. Ed*, 2014, **53**, 5427-5430.
10. J. Tian, Q. Liu, A. M. Asiri and X. Sun, *J. Am. Chem. Soc.*, 2014, **136**, 7587-7590.
11. C. Zhang, Y. Huang, Y. Yu, J. Zhang, S. Zhuo and B. Zhang, *Chem. Sci.*, 2017, **8**, 2769-2775.
12. Z. H. Xue, H. Su, Q. Y. Yu, B. Zhang, H. H. Wang, X. H. Li and J. S. Chen, *Adv. Energy Mater.*, 2017, **7**, 1602355.
13. J. Tian, Q. Liu, N. Cheng, A. M. Asiri and X. Sun, *Angew. Chem. Int. Ed.*, 2014, **53**, 9577-9581.
14. P. Jiang, Q. Liu, Y. Liang, J. Tian, A. M. Asiri and X. Sun, *Angew. Chem. Int. Ed.*, 2014, **53**, 12855-12859.
15. S. Han, Y. Feng, F. Zhang, C. Yang, Z. Yao, W. Zhao, F. Qiu, L. Yang, Y. Yao, X. Zhuang and X. Feng, *Adv. Funct. Mater.*, 2015, **25**, 3899-3906.
16. Y. Liang, Q. Liu, A. M. Asiri, X. Sun and Y. Luo, *ACS Cata.*, 2014, **4**, 4065-4069.
17. J. Kibsgaard and T. F. Jaramillo, *Angew. Chem. Int. Ed.*, 2014, **53**, 14433-14437.
18. Y. Pan, Y. Liu, J. Zhao, K. Yang, J. Liang, D. Liu, W. Hu, D. Liu, Y. Liu and C. Liu, *J. Mater. Chem. A*, 2015, **3**, 1656-1665.
19. Z. Huang, Z. Chen, Z. Chen, C. Lv, H. Meng and C. Zhang, *ACS Nano*, 2014, **8**, 8121-8129.
20. T. Tian, L. Ai and J. Jiang, *RSC Adv.*, 2015, **5**, 10290-10295.
21. Z. Pu, Q. Liu, A. M. Asiri and X. Sun, *ACS Appl. Mater. Interfaces*, 2014, **6**, 21874-21879.